

# Influence of methyl red as a dopant on the electrical properties and device performance of liquid crystals

Po-Chang Wu,<sup>1</sup> Chien-Tsung Hou,<sup>2</sup> Yu-Cheng Hsiao,<sup>1</sup> and Wei Lee<sup>1,2,\*</sup>

<sup>1</sup>*Institute of Imaging and Biomedical Photonics, College of Photonics, National Chiao Tung University, Guiren Dist., Tainan 71150, Taiwan*

<sup>2</sup>*Department of Physics, Chung Yuan Christian University, Chungli 32023, Taiwan*  
[wlee@nctu.edu.tw](mailto:wlee@nctu.edu.tw)

**Abstract:** The ionic effect in nematic liquid-crystal (LC) cells containing the azo dye methyl red was investigated by means of dielectric spectroscopy, measurements of voltage holding ratio (VHR) and ultraviolet/visible absorption spectroscopy. The experimental results indicated that incorporating a minute amount of the methyl red (< 0.03 wt%) in the LC host leads to the suppression of the ionic effect caused by impurity ions. Practically, the doped LC cells with a dye content of 0.02 wt% showed improved VHR and promoted lifetime by 15% and 180%, respectively, in virtually no expense of the optical transmittance.

©2014 Optical Society of America

**OCIS codes:** (160.3710) Liquid crystals; (160.4890) Organic materials; (230.3720) Liquid-crystal devices.

---

## References and links

1. N. Sasaki, "Simulation of the voltage holding ratio in liquid crystal displays with a constant charge model," *Jpn. J. Appl. Phys.* **37**(11), 6065–6070 (1998).
2. T. Nakanishi, T. Takahashi, H. Mada, and S. Saito, "Transient behavior of voltage holding ratio in nematic liquid crystal cells," *Jpn. J. Appl. Phys.* **41**(Part 1, No. 6A), 3752–3757 (2002).
3. M. Mizusaki, Y. Yoshimura, Y. Yamada, and K. Okamoto, "Analysis of ion behavior affecting voltage holding property of liquid crystal displays," *Jpn. J. Appl. Phys.* **51**(1R), 014102 (2012).
4. H. D. Vleeschouwer, A. Verschuereen, F. Bougrioua, K. Neyts, G. Stojmenovic, S. Vermael, and H. Pauwels, "Dispersive ion generation in nematic liquid crystal displays," *Jpn. J. Appl. Phys.* **41**(Part 1, No. 3A), 1489–1494 (2002).
5. S. Murakami and H. Naito, "Charge injection and generation in nematic liquid crystal cells," *Jpn. J. Appl. Phys.* **36**(2), 773–776 (1997).
6. W. Lee, C.-Y. Wang, and Y.-C. Shih, "Effects of carbon nanosolids on the electro-optical properties of a twisted nematic liquid-crystal host," *Appl. Phys. Lett.* **85**(4), 513–515 (2004).
7. H.-Y. Chen and W. Lee, "Suppression of field screening in nematic liquid crystals by carbon nanotubes," *Appl. Phys. Lett.* **88**(22), 222105 (2006).
8. B.-R. Jian, C.-Y. Tang, and W. Lee, "Temperature-dependent electrical properties of dilute suspensions of carbon nanotubes in nematic liquid crystals," *Carbon* **49**(3), 910–914 (2011).
9. C.-W. Lee and W.-P. Shih, "Quantification of ion trapping effect of carbon nanomaterials in liquid crystals," *Mater. Lett.* **64**(3), 466–468 (2010).
10. P.-S. Chen, C.-C. Huang, Y.-W. Liu, and C.-Y. Chao, "Effect of insulating-nanoparticles addition on ion current and voltage-holding ratio in nematic liquid crystal cells," *Appl. Phys. Lett.* **90**(21), 211111 (2007).
11. C.-Y. Tang, S.-M. Huang, and W. Lee, "Electrical properties of nematic liquid crystals doped with anatase TiO<sub>2</sub> nanoparticles," *J. Phys. D Appl. Phys.* **44**(35), 355102 (2011).
12. H.-H. Liu and W. Lee, "Time-varying ionic properties of a liquid-crystal cell," *Appl. Phys. Lett.* **97**(2), 023510 (2010).
13. H.-H. Liu and W. Lee, "Ionic properties of liquid crystals dispersed with carbon nanotubes and montmorillonite nanoplatelets," *Appl. Phys. Lett.* **97**(17), 173501 (2010).
14. S.-W. Liao, C.-T. Hsieh, C.-C. Kuo, and C.-Y. Huang, "Voltage-assisted ion reduction in liquid crystal-silica nanoparticle dispersions," *Appl. Phys. Lett.* **101**(16), 161906 (2012).
15. H.-J. Kim, Y.-G. Kang, H.-G. Park, K.-M. Lee, S. Yang, H.-Y. Jung, and D.-S. Seo, "Effects of the dispersion of zirconium dioxide nanoparticles on high performance electro-optic properties in liquid crystal devices," *Liq. Cryst.* **38**(7), 871–875 (2011).

16. H.-M. Lee, H.-K. Chung, H.-G. Park, H.-C. Jeong, J.-J. Han, M.-J. Cho, J.-W. Lee, and D.-S. Seo, "Residual DC voltage-free behaviour of liquid crystal system with nickel nanoparticle dispersion," *Liq. Cryst.* **41**(2), 247–251 (2014).
17. A. Y.-G. Fuh, C. C. Liao, K. C. Hsu, and C. L. Lu, "Laser-induced reorientation effect and ripple structure in dye-doped liquid-crystal films," *Opt. Lett.* **28**(14), 1179–1181 (2003).
18. A. Y.-G. Fuh, C.-K. Liu, K.-T. Cheng, C.-L. Ting, C.-C. Chen, P. C.-P. Chao, and H.-K. Hsu, "Variable liquid crystal pretilt angles generated by photoalignment in homeotropically aligned azo dye-doped liquid crystals," *Appl. Phys. Lett.* **95**(16), 161104 (2009).
19. K.-Y. Yang and W. Lee, "Voltage-assisted photoaligning effect of an azo dye doped in a liquid crystal with negative dielectric anisotropy," *Opt. Express* **18**(19), 19914–19919 (2010).
20. H. Akiyama, T. Kawara, H. Takada, H. Takatsu, V. Chigrinov, E. Prudnikova, V. Kozenkov, and H. Kwok, "Synthesis and properties of azo dye aligning layers for liquid crystal cells," *Liq. Cryst.* **29**(10), 1321–1327 (2002).
21. V. Chigrinov, A. Muravski, H.-S. Kwok, H. Takada, H. Akiyama, and H. Takatsu, "Anchoring properties of photoaligned azo-dye materials," *Phys. Rev. E Stat. Nonlin. Soft Matter Phys.* **68**(6), 061702 (2003).
22. M. Okutan, S. E. San, O. Köysal, and E. Şentürk, "The electrical properties of a fullerene and C.I. Acid Red 2 (methyl red) doped E7 nematic liquid crystal," *Dyes Pigments* **84**(3), 209–212 (2010).
23. M. Rahman, C.-W. Hsieh, C.-T. Wang, B.-R. Jian, and W. Lee, "Dielectric relaxation dynamics in liquid crystal – dye composites," *Dyes Pigments* **84**(1), 128–133 (2010).
24. C.-Y. Tang, S.-M. Huang, and W. Lee, "Dielectric relaxation dynamics in a dual-frequency nematic liquid crystal doped with C.I. Acid Red 2," *Dyes Pigments* **88**(1), 1–6 (2011).
25. P. Perkowski, "Dielectric spectroscopy of liquid crystals. Theoretical model of ITO electrodes influence on dielectric measurements," *Opto-Electron. Rev.* **17**(2), 180–186 (2009).
26. G. Barbero, A. L. Alexe-Ionescu, and I. Lelidis, "Significance of small voltage in impedance spectroscopy measurements on electrolytic cells," *J. Appl. Phys.* **98**(11), 113703 (2005).
27. P.-C. Wu and W. Lee, "Phase and dielectric behaviors of a polymorphic liquid crystal doped with graphene nanoplatelets," *Appl. Phys. Lett.* **102**(16), 162904 (2013).
28. F.-C. Lin, P.-C. Wu, B.-R. Jian, and W. Lee, "Dopant effect and cell-configuration- dependent dielectric properties of nematic liquid crystals," *Adv. Cond. Mat. Phys.* **2013**, 271574 (2013).
29. X. Ma and M. Zhou, "A comparative study of azo dye decolorization by electro-Fenton in two common electrolytes," *J. Chem. Technol. Biotechnol.* **84**(10), 1544–1549 (2009).
30. L. Lucchetti and F. Simoni, "Role of space charges on light-induced effects in nematic liquid crystals doped by methyl red," *Phys. Rev. E Stat. Nonlin. Soft Matter Phys.* **89**(3), 032507 (2014).

## 1. Introduction

Liquid-crystal display (LCD) is the most common application among all LC-based electro-optical devices. Nowadays, LCDs are extensively utilized in various information-content products such as televisions, monitors, digital cameras and mobile phones. As the demands for image quality increase and the green concept emerges readily in electronic products, LCDs with low power consumption and high definition image are strongly desired. However, owing to the unavoidable impurity ions presenting in the LCD the ionic effect has long been a crucial problem to degrade display properties, such as increased threshold voltage, prolonged response time, and worsened image quality and stability. The ionic effect stems from not only the transport behavior of impurity ions in the bulk but the adsorption of ions from the surfaces of alignment layers and electrodes in a cell. Upon application of an applied voltage to the cell, the transportation of ions in response to the electric field leads to the formation of electrode-double layers near the electrodes and, in turn, to the decrease in effective voltage applied across the LC layer. The voltage holding ratio (VHR), defined as the fraction of the residual voltage after a certain duration in open circuit to the initially applied voltage, is one of the most important parameters for determining the performance of an LCD, in which a sufficiently high VHR gives rise to high reliability of image quality with uniform contrast ratio and stable image without flicker. It has long been established that the presence of impurity ions leads to the reduction in VHR due to the transport of ions in the LC cell under an applied voltage [1–3]. As the unwanted ionic effect can hardly be avoided completely in the LCD, adopting a LC material with high resistivity and low ionic concentration is a direct way for obtaining high VHR. However, the ionic concentration could further ascend owing to the dissociation of the LC material and ion-injection from the alignment or electrode layers in the cell [4,5]. Recently, dilute dispersions of nanoscale additives in LCs have been proven as an effective and non-synthetic approach to suppression of the ionic effect. Based on revealed material features, it has been demonstrated that specific types of *inorganic* nanomaterials,

such as carbon-based allotropes [6–9] (including diamond powders [10]), TiO<sub>2</sub> [11], clay platelets [12,13] SiO<sub>2</sub> [14], semiconductor ZnO [15] and ferromagnetic nickel nanoparticles [16], doped in LC cells enable the trapping of ion impurities and, in turn, the reduction in ionic concentration. As a result, rectification of display performance, including lowered threshold voltage, shortened response time and increased VHR, has been clarified using these LC–nanosolid colloids. Unfortunately, long-term colloidal stability in such organic–inorganic hybrid suspensions is always a big challenge for further applications to LCD products because the solutes often aggregate over time through the intrinsic interparticulate interaction and the ordering of LC mesophases.

In view of the limitation of inorganic solids, *organic* additives certainly play a crucial role in display performance. For instance, chiral dopants are ubiquitously found in twisted–nematic LCDs for boosting the electro-optical response speed. Dichroic dyes such as methyl red (MR) are photo-sensitive organic materials having spectral features of absorbing specific wavelengths of light. Due to their superior miscibility with LCs, organic dyes, in comparison with inorganic nanosolids, warrant the desired colloidal stability and, hence, reliability of the resulting LC mixture. Investigations of the control of the orientation as well as pretilt angle of LC molecules in dye-doped LC cells have been reported based on the light-induced *trans*-to-*cis* isomerization [17–19]. In addition, other studies have confirmed that some azo dyes serving as alignment layers in LC cells cannot only dictate the orientation of LC molecules but also result in a higher VHR in comparison with that of a typical cell with conventional rubbed polyimide alignment layers coated on the cell substrates [20,21]. Although there exist documents in the literature concerning the dielectric relaxation dynamics in dye-doped LC cells [22–24], most of them are reported in the high-frequency regime ( $f > 100$  kHz) where no ionic effect dominates the dielectric relaxation, thus giving no information on the field screening caused by impurity ions.

In this study, we considered an azo-dye-doped LC composite system and obtained the low-frequency dielectric spectra as well as the VHR data to investigate the dopant effect on the behavior of impurity ions in the LC cells. The spectra of the dielectric complex function in low frequencies, characterized by the space-charge polarization, were used to deduce the ionic behavior in the cells. Further comparison of VHR between the dye-doped cells and the pristine counterpart disclosed evident depression of ions by the azo additive. We measured the time-evolved VHR and established a lifetime parameter to evaluate the time-varying VHR property of the LC cells. The mechanisms underlying the promoted device performance by the azo dye are suggested. On the other hand, it is well known in the LCD industry that the ubiquitous ultraviolet (UV) light is one of the negative environmental factors to degrade the performance of a LCD. Considering the impact of environmental conditions on the integrity of a LC cell, the effect of UV-light illumination on the ionic behavior of both pure and dye-doped LC cells is discussed.

## 2. Experiment

The LC material used in this study was E7 (Merck), a eutectic mixture having high concentration of impurity ions and low resistivity ( $\sim 10^{11}$   $\Omega\cdot\text{cm}$ ). It consists of four compounds, 4'-*n*-pentyl-4-cyanobiphenyl (5CB), 4'-*n*-heptyl-4-cyanobiphenyl (7CB), 4'-*n*-octyloxy-4-cyanobiphenyl (8OCB) and 4'-*n*-pentyl-4-cyano-*p*-triphenyl (5CT). The dichroic azo dye 2-[[4-(dimethylamino)phenyl]diazenyl]benzoic acid, better known as MR with the molecular formula C<sub>15</sub>H<sub>15</sub>N<sub>3</sub>O<sub>2</sub>, was purchased from Sigma–Aldrich and used as received. The molecular structures of E7 and MR are illustrated in Fig. 1. Under no considerable stimuli such as widely used, polarized laser beams with wavelengths in the light-absorption range of the MR molecules and the UV irradiation discussed in this study to extensively activate the *trans*-to-*cis* isomerization, the majority of the MR molecules were ideally stabilized in the *trans* state with their molecular axes parallel to the LC director. The mixtures were prepared with MR concentrations ranging from 0.01 to 0.50 wt%. The dye-doped and pristine E7 samples were introduced by the capillary action into commercially available planar-alignment cells purchased from Mesostate LCD Industries Co., Ltd; thus, the orientations of the LC and

dye molecules were practically parallel to the substrate plane. Except for the cell gap and electrode area, all cells were made using identical alignment films of SE-2170 (Nissan Chem. Co.) and indium–tin-oxide (ITO)-coated glass substrates with resistance of  $\sim 140 \Omega/\square$  [8]. In this work, two series of samples with two designated cell gaps and electrode areas were prepared to carry out two independent experiments. The cells used for experiments without UV exposure, including measurements of the VHR and the dielectric and transmission spectra, have an electrode area  $A = 1.0 \text{ cm}^2$  and a cell gap  $d = 5.9 \pm 0.5 \mu\text{m}$ . With a finite voltage regime of an arbitrary function generator, the LC cells with  $d = 5.9 \pm 0.5 \mu\text{m}$  are applicable to ensure complete reorientation of LC molecules from the planar to homeotropic state under an applied voltage in the measurement of VHR. Without enough quantity of the empty cells of this type, the later experiment concerning the UV effect on the dielectric dispersion of both dye-doped and undoped LC samples were acquired using another type of cells with  $A = 0.25 \text{ cm}^2$  and  $d = 12 \pm 0.5 \mu\text{m}$ . Although the reason for the use of distinct cells in this work originates from the limited quantity of empty cells available in our laboratory, the larger electrode area and smaller cell gap of a cell, regarded as a “larger” capacitor, affect primarily on the complex dielectric function in the high-frequency regime, attributable to the ITO effect that leads to the induced pseudo-relaxation [25]. Consequently, in considering the effect of cell configuration on the dielectric spectrum of a LC cell, it is worth mentioning that once the samples with identical aligning and electrode materials were used for dielectric measurements, the resulting dielectric spectra of cells are meaningful for investigating the dopant effect of MR on the ionic behavior.

Three types of experiments, dielectric spectroscopy, the VHR measurement and ultraviolet/visible absorption spectroscopy, were carried out at room temperature. The complex dielectric spectra in the frequency regime between  $10^{-1}$  and  $10^4$  Hz were acquired using a high-precision LCR (inductance–capacitance–resistance) meter (HIOKI 3522-50). The probe voltage was  $0.5 \text{ V}_{\text{rms}}$  in the sinusoidal waveform, which was smaller than the Fréedericksz-transition voltage of the LC. Since the used probe voltage is somewhat higher than the thermal voltage defined as  $V_T = k_B T/q \approx 0.025 \text{ V}$ , where  $k_B$  is the Boltzmann constant,  $T$  is the absolute temperature and  $q$  is the charge of an ion, the ionic behavior in the low-frequency regime investigated is possible to be nonlinear [26]. In this case, the voltage used is sufficient to perturb the distribution of ions with parts of charges being polarized, meaning that the analysis on detailed ionic properties becomes more complicated. Unfortunately, it is unpractical to adopt a lower probe voltage for experiments due to the limit of the instrument (i.e., the used LCR meter) of  $0.05 \text{ V}_{\text{rms}}$  as well as the signal-to-noise ratio. Although the detailed analysis on the dielectric data is restricted by such a nonlinear manner in our system, once the samples with identical cell parameters including thickness and electrode area were used for each dielectric measurement, the investigated dielectric spectra of cells are still meaningful for investigating the dopant effect of MR on the ionic behavior from the big picture.

On the other hand, the VHR, simulating the charge and discharge behaviors in a LC cell, is a useful measure of the device performance of the LCD. The VHR is defined as [11]

$$\text{VHR (\%)} = \left( \frac{V_t}{V_i} \right) \times 100\%, \quad (1)$$

where  $V_i$  and  $V_t$  denote the input and terminal voltages during a frame time, respectively. The data line was  $5 \text{ V}$  in the square waveform with a frame time of  $16.67 \text{ ms}$  (corresponding to a frequency of  $60 \text{ Hz}$ ), and the pulse width of the scan line was  $15.6 \mu\text{s}$  at  $60 \text{ Hz}$ . Both data-line and scan-line signals were supplied by an arbitrary function generator (Tektronix AFG-3022B). Besides, the transmission spectra in the wavelength range from  $380$  to  $780 \text{ nm}$  were measured with a high-speed fiber-optic spectrometer (Ocean Optics HR2000 + ) in conjunction with a halogen light source (Ocean Optics HL2000).

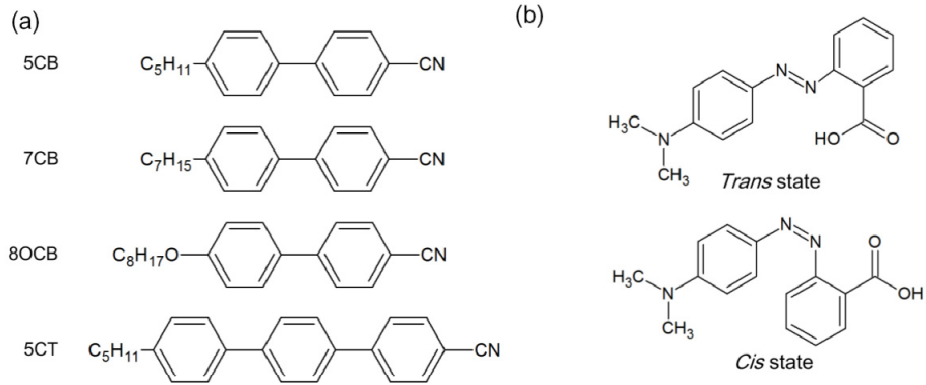


Fig. 1. Molecular structures of (a) the constituent compounds of the LC E7 and (b) the azo dye MR in the *trans* and *cis* states.

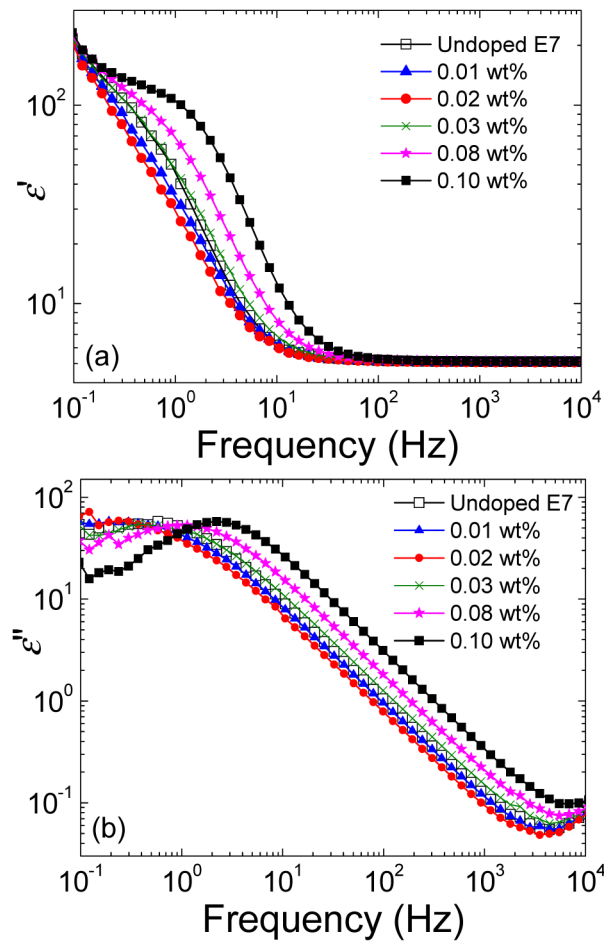


Fig. 2. The dielectric spectra of the (a) real-part and (b) imaginary-part dielectric functions of undoped and doped E7 cells with different contents of MR.

### 3. Results and discussion

Figure 2 depicts the dielectric spectra of LC cells with various MR contents in comparison with an undoped E7 counterpart. The complex dielectric function is defined as  $\epsilon^* = \epsilon' - i\epsilon''$ , where  $\epsilon'$  and  $\epsilon''$  represent the real and imaginary parts of dielectric permittivity, respectively. Here, the space-charge polarization can clearly be observed in the frequency regime between 0.1 and 100 Hz in all cells, with the real ( $\epsilon'$ ) and imaginary parts ( $\epsilon''$ ) of the frequency ( $f$ )-dependent dielectric function being inversely proportional to  $f^{3/2}$  and  $f$ , respectively [27]. Compared with pure E7, one can see from Fig. 2 that, as the dye concentration increased, both  $\epsilon'$  and  $\epsilon''$  in this frequency range decreased in the lightly doped (0.01 and 0.02 wt%) LC cells, reaching minima for the 0.02 wt% sample, and then became larger than those of the pure counterpart as the dye content went beyond 0.03 wt%. The smaller the electric susceptibility, the lower the extent of a material to be polarized in response to a given field. The reduced values of  $\epsilon'$  and  $\epsilon''$  thus indicate the weakened ionic effect in the lightly doped cells accordingly. Consider a general LC cell having an alignment film and a fixed electrode area coated on each glass substrate, the ionic effect in the investigated frequency regime is attributable to not only the transport of ions in the bulk but the absorption/desorption behavior of ions near the surfaces of alignment films and electrodes. Because both the aligning and electrode materials used are identical for all samples, the contributions of ion-absorption from the surfaces and the character of the electrodes to the ionic effect are fixed. Accordingly, it is reasonable to preliminarily imply that MR in a minute amount dispersed in LC cells can depress the ion transport. In view of the molecular structure of the dye, as shown in Fig. 1(b), the mechanisms for the observed ion suppression can be derived based on the following reasons: First, the nitrogen atoms having unpaired electrons in the MR molecule tend to adsorb positive ions such as magnesium, calcium and zinc, which are commonly found in ion-rich LCs such as E7, and then form ligand covalent bond and metal complexes, thereby weakening the field-screening effect caused by metal impurity ions. The other reasonable speculation is that hydrons from the carboxyl side would move to the methyl side in MR molecules through the electrochemical effect near the electrode surfaces, rendering immobilized ion impurities in the LC bulk by interaction with the resulting dipole moment. Furthermore, by taking into account the unique feature of MR adsorption onto the surface, it is likely that, when free space charges in responding to the probe ac voltage migrate to the surfaces, the MR molecules restrain the ion transport or even trap ions near substrate surfaces, leading to the depressed ionic effect observed in the MR-doped LC cell. Note that the overdose of MR would be regarded as “impurity ions” when the dye concentration rises to 0.03 wt% and above (see Fig. 2).

From the point of view of practical applications in displays, Fig. 3 shows the comparison of VHR between the undoped and 0.02 wt%-doped LC cells. It is obvious that impregnating MR dye in the cell enabled the VHR to increase from 64.8 to 74.4%, yielding a promotion by 15%. This result connotes the restrain of ion transport by the MR dye. Since organic dyes from point of view of material compatibility are more mixable with LCs, it is believed using MR dye instead of inorganic nanomaterials for the suppression of ionic effect in a LC cell is more reliable and applicable for practical uses. Furthermore, Fig. 4 displays the time-evolved VHR of both the 0.02 wt%-doped and undoped LC cells. The decrease in VHR for both cells with increasing time can be explained by the rising ionic concentration after cell fabrication [12]. Considering the variation of VHR within five days, one can see that the values of VHR for the doped and undoped cells in five days (120 h) dropped by *ca.* 14% and 35%, respectively, compared with those of the cells at 0 h. In addition, the attrition rate of a LC cell through prolonged operation can be monitored via the lifetime parameter  $\tau$ , following the monoexponential decay expression:

$$\text{VHR}(t) = A \exp\left(\frac{-t}{\tau}\right), \quad (2)$$

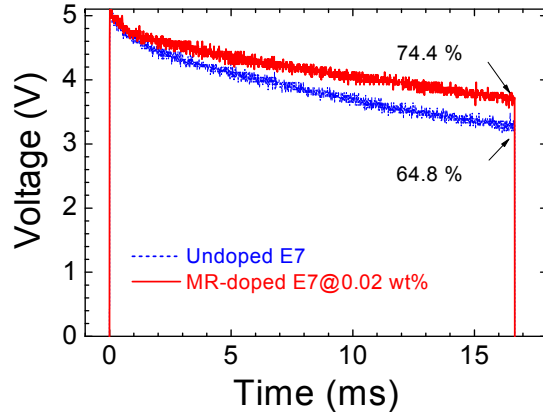


Fig. 3. Voltage responses and calculated VHR of undoped and doped E7 cells.

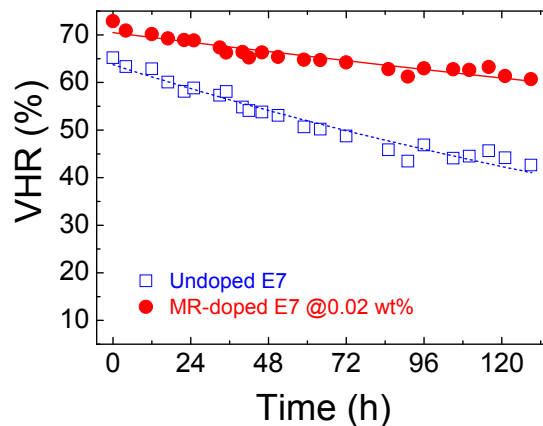


Fig. 4. Time-evolved VHR of undoped and doped E7 cells. The curves are exponentially fitted to the experimental data.

where  $A$  is the VHR at time  $t = 0$ . Results from fitting experimental data demonstrated that the lifetime was greatly improved by 180%—from 294 h for the undoped cell to 823 h (i.e., 2.8 times larger) for the doped one. Apparently, the addition of MR in E7 enhanced the VHR stability and extended the cell lifetime.

To observe the UV effect on the ionic behavior in dye-doped LC cells, Fig. 5 shows the ion density  $n$  and diffusivity  $D$  varying with the time of UV-light illumination. Here, the wavelength and strength of UV light are 365 nm and  $0.2 \text{ mW/cm}^2$ , respectively. The values of  $n$  and  $D$  are deduced by fitting the experimental data of complex dielectric functions of the  $12\text{-}\mu\text{m}$  cells in appropriate frequency ranges according to the model established especially for studying the ionic behavior in LCs [28]. In Fig. 5, the rise in  $D$  with increasing UV-exposure time in each cell indicates the promoted ionic effect stemming partly from the dissociation of the LC molecules under UV irradiation. For the dye-doped LC cells, it can be suggested from the preliminary experiments that the UV exposure enables the transformation of dye molecules from the stable *trans* to *cis* state via photoinduced *trans*-to-*cis* isomerization; thus, leading to the reduction in LC ordering and the overall resistivity in the dyed LC systems. Referring to relevant studies concerning light effect of MR-doped LCs in the literature, one may not directly perceive the *trans*-to-*cis* isomerization by UV irradiation since the maximum absorption in the visible spectrum of the MR dye is at nearly 500 nm as shown in Fig. 6. While considering the general concept of molecular spectroscopy, the MR molecules having

two benzenoid rings do absorb UV light, ascribed to the absorption of the  $\pi \rightarrow \pi^*$  transition [29]. In addition to the green light absorption, this UV absorption route becomes another means for photoisomerization. On the other hand, since the MR molecules form charge complexes on the surface, it has recently been established that the change in surface anchoring energy and the LC orientation by light irradiation originate from the light-induced absorption/desorption of not only the MR molecules but the formed charge complexes as well [30]. Based on this mechanism, it is reasonable to say that the increase in  $n$  and  $D$  with increasing UV-exposure time in the dye-doped LC cells is attributable to the modified LC ordering and the desorption of charges from the surfaces. Particularly, in the absence of UV-light irradiation, the values of  $n$  and  $D$  in the 0.02-wt%-MR-doped LC cell are 6 and 28% lower than those of the pure counterpart, respectively. This confirms the preliminary interpretation for those results shown in Fig. 2. It further indicates that a trace amount of MR dyes doped in LCs is more sufficient to restrain ion transport rather than to trap ions. Once exposed to UV light, both the values of  $n$  and  $D$  in doped LC with 0.02 wt% of MR becomes comparable to that of the pure LC cell as the exposure time goes beyond 120 min. It is likely that the ability of MR molecules for ion-trapping vanishes as the molecular state changes from the *trans* state to the *cis* state. This also implies that, compared with that of the reference (i.e., undoped) cell, the kinetic energy of ions does not increase apparently in doped cells with dye concentrations lower than 0.02 wt% even under reasonable UV illumination.

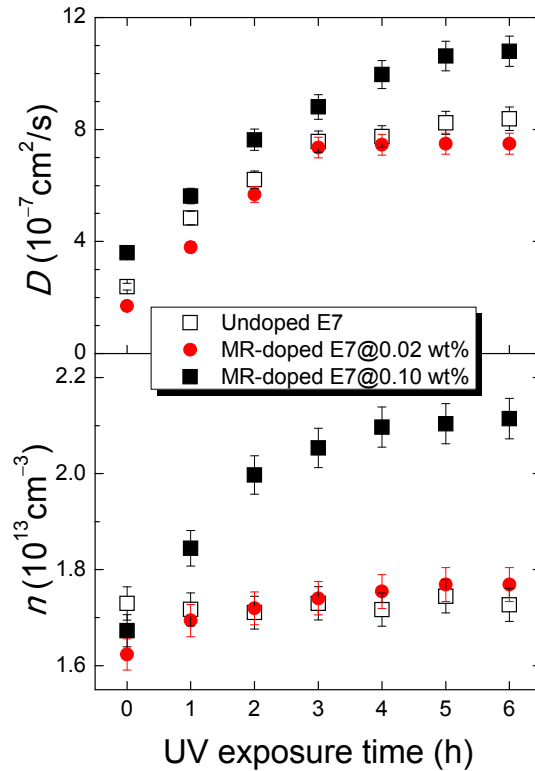


Fig. 5. Deduced ion density  $n$  and diffusivity  $D$  in undoped and MR-doped E7 cells under UV exposure.



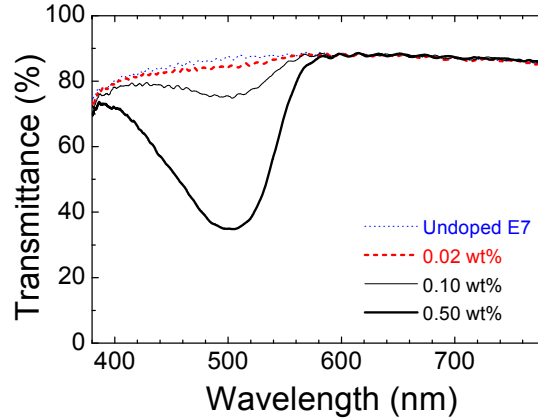


Fig. 6. Transmission spectra of undoped and doped E7 cells with different contents of MR dye.

Figure 6 shows the transmission spectra of the undoped and MR-doped E7 cells without performing UV exposure. Note that none of any polarizer was employed in this measurement. For an unpolarized white light passing through a MR-doped LC cell, the MR dye absorbs the green and blue light according to its material feature. Increasing the dopant concentration of the MR leads to the promotion in light absorption for the dye-doped LC system. As a consequence, the apparent drop in transmittance in the spectral range between 400 and 600 nm for dye-doped cell with MR content of either 0.1 or 0.5 wt% results from considerable amounts of MR dyes doped in the LC cells. Notably, Fig. 6 delineates a nearly unchanged transmission spectrum of the 0.02 wt%-doped cell with respect to the pure E7 counterpart. The 2% decrease in transmittance at the wavelength of peak absorption near 500 nm is completely negligible for a full-color LC device (with 380–780 nm taken into account). It is worth noting that a trace amount of MR dye can suppress the impurity ions and, in turn, improve the VHR and its long-term stability without sacrificing the transmittance.

#### 4. Conclusions

In conclusion, the dopant effect of MR on the ionic effect in LC cells has been investigated. Both the low-frequency dielectric spectra and the VHR have been measured for discussion of the ionic behavior in the cells. From the data of the dielectric spectra in the frequency range between 0.1 and 100 Hz, the doped E7 cell with MR content of 0.02 wt% showed the lowest dielectric loss among all cells studied, indicating the best condition on suppressing impurity ions. Based on this result, we further compared the VHR between the undoped and doped E7 cell with 0.02 wt% and established a characteristic lifetime as a measure of the long-term stability in VHR of a cell. We demonstrated that the VHR and lifetime constant were improved by, respectively, 15% and 180% for the MR-doped cell. While considering the practical application of this dye/LC hybrid structure, our results implied that the device performance can be enhanced by a minute addition of MR dye without appreciably surrendering transmittance of the LC cell. Our findings thus open up a possible approach to repressing the ionic effect in a LC cell. Selected dye materials for depressing ions and balancing the color gamut should be considered to improve the performance in general LCD technologies. Alternatively, using specific molecules having no absorption in the visible range as an ion-suppressor in LCs would be practical to promote the display performance while retaining its optical transmittance.

#### Acknowledgments

This work was financially supported by the Ministry of Science and Technology, Taiwan, through grant Nos. 101-2112-M-009-018-MY3 and 102-2811-M-009-060.